Analysis of a Gas Circuit Breaker Using the Fast Moving Least Square Reproducing Kernel Method

Chany Lee*, Do Wan Kim, Sang-Hun Park***, Hong-Kyu Kim*** and Hyun-Kyo Jung***

Abstract – In this paper, the arc region of a gas circuit breaker (GCB) is analyzed using the fast moving least square reproducing kernel method (FMLSRKM) which can simultaneously calculate an approximated solution and its derivatives. For this problem, an axisymmetric and inhomogeneous formulation of the FMLSRKM is used and applied. The field distribution obtained by the FMLSRKM is compared to that of the finite element method. Then, a whole breaking period of a GCB is simulated, including analysis of the arc gas flow by finite volume fluid in the cell, and the electric field of the arc region using the FMLSRKM.

Keywords: Fast moving least square reproducing kernel method (FMLSRKM), Gas circuit breaker (GCB), Meshfree, Meshless

1. Introduction

To calculate the breaking performance of a gas circuit breaker (GCB), the electric field in an arc region of a GCB should be analyzed [1]. It is an inhomogeneous problem due to the fact irregular distributions of pressure and temperature in the arc region cause inhomogeneous electric conductivity [2]. Moreover, because of the geometry of the GCB and the heavy load of a 3-dimensional calculation, it needs to be treated as an axisymmetric problem [1], [2].

The fast moving least square reproducing kernel method (FMLSRKM) is a kind of meshfree method studied by many researchers [3]-[10]. The FMLSRKM is able to solve a variety of problems, including Poisson, stationary incompressible Stokes, and many electromagnetic problems [3], [4]. As with other meshfree methods, such as smoothed particle hydrodynamics (SPH) [5], the element free Galerkin method (EFG) [6], the moving least square reproducing kernel method (MLSRKM) [7], and so on [3], [8], [9], FMLSRKM does not require a mesh generation process. Moreover, the refinement scheme of a meshfree method is simpler than that of a finite element method (FEM) as all that is required is for additional nodes to be placed in high-error regions [10].

For accurate approximation of meshfree methods, a high order basis function is required. Furthermore, in cases using a point collocation scheme as a meshfree method, higher order derivatives are needed. Consequently, the calculation of an approximated solution and its derivatives is unavoidable, but obtaining these derivatives makes meshfree methods computationally heavy. However, the FMLSRKM not only gives an approximated solution, but also high order approximated derivatives up to the order of the basis polynomials, simultaneously [3]. Therefore, this method is adopted in this work for fast calculation.

In this paper, the FMLSRKM point collocation formulation for an axisymmetric and inhomogeneous problem is shown. In addition, we briefly explain a way to analyze an arc gas flow in a GCB. Then, simulation results are also represented.

2. Method

2.1 FMLSRKM

The FMLSRKM is able to produce an approximated solution u^h at $\mathbf{x}$ near $\bar{\mathbf{x}}$ can be determined using polynomial bases, like

$$u^h(\mathbf{x},\bar{\mathbf{x}}) = \mathbf{P}_m(\frac{\mathbf{x}-\bar{\mathbf{x}}}{\rho}) \bullet \mathbf{a}(\bar{\mathbf{x}}), \tag{1}$$

where, $\mathbf{P}_m$ is the complete basis polynomial vector up to order m, $\mathbf{a}(\bar{\mathbf{x}})$ is the unknown coefficient vector for the local area of $\bar{\mathbf{x}}$ [4]-[6]. In this paper, $\mathbf{x}=[r\ z]^T$ because the problem is axisymmetric, and ρ is the dilation parameter, which represents the region of influence of $u^h(\mathbf{x},\bar{\mathbf{x}})$. In order to obtain the coefficient vector $\mathbf{a}(\bar{\mathbf{x}})$, the moving least square scheme is applied. Some mathematics (detailed in [4], [5]) lead to

$$u^h(\mathbf{x},\bar{\mathbf{x}}) = \mathbf{P}_m^T(\frac{\mathbf{x}-\bar{\mathbf{x}}}{\rho})\ M^{-1}(\bar{\mathbf{x}}) \times \sum_{I=1}^{NP} \mathbf{P}_m(\frac{\mathbf{x}_I-\bar{\mathbf{x}}}{\rho})\Phi_\rho(\mathbf{x}_I-\bar{\mathbf{x}})u(\mathbf{x}_I), \tag{2}$$

* School of Electrical Engineering and Computer Science, Seoul National University, Korea. (chany@elecmech.snu.ac.kr, hkjung @snu.ac.kr)
** Department of Applied Mathematics, Hanyang University, Korea. (dokim@hanyang.ac.kr)
*** Korea Electrotechnology Research Institute (KERI), Korea (echo@keri.re.kr, kimhk@keri.re.kr).
Received 12 November 2008; Accepted 21 January 2009

$$M(\bar{\mathbf{x}}) = \sum_{I=1}^{NP} \mathbf{P}_m(\frac{\mathbf{x}_I - \bar{\mathbf{x}}}{\rho})\mathbf{P}_m^T(\frac{\mathbf{x} - \bar{\mathbf{x}}}{\rho})\Phi_\rho(\mathbf{x}_I - \bar{\mathbf{x}}), \quad (3)$$

where, NP is the number of nodes in the local area, and

$$\Phi_\rho(\mathbf{x}_I - \bar{\mathbf{x}}) = (1/\rho^2)\Phi(\frac{\mathbf{x}_I - \bar{\mathbf{x}}}{\rho}). \quad (4)$$

is called the window function, where

$$\Phi(\mathbf{x}) = \begin{cases} (1 - \|\mathrm{x}\|)^t, & \text{when } \|\mathrm{x}\| < 1,\ t > 0 \\ 0, & \text{otherwise.} \end{cases}$$

2.2 Analysis of Electric Field on the Arc Region

As mentioned above, the arc region of a GCB can be treated as an axisymmetric problem with inhomogeneous electric conductivity [1], [2]. Hence, development of the FMLSRKM formulation for this problem is required. In a GCB, an arc is generated in the arc region between two electrodes, such as in Fig. 1. The arc region Ω is shown in the bottom left of Fig. 1. This arc region is governed by Ohm's law and the equation of continuity like

$$\vec{J} = \sigma\vec{E}, \quad (5)$$

$$\nabla \bullet \vec{J} = 0, \quad (6)$$

where, $\vec{J}$ is the electric current density, $\vec{E}$ is the electric field intensity, and σ is the electric conductivity. So, the electric potential ϕ can be expressed as

$$\nabla \bullet (\sigma\nabla\phi) = 0 \quad \text{in } \Omega, \quad (7)$$

and boundary conditions are given such as

$$\phi = g, \qquad \text{on } \Gamma_D \quad (8)$$

$$\frac{\partial\phi}{\partial n} = h, \qquad \text{on } \Gamma_N \quad (9)$$

[1]-[3]. Dirichlet boundary conditions are applied at the interfaces between the electrodes and the arc region denoted as the bottom right of Fig.1, and its values are set to ϕ_a = 1V, ϕ_b = 0V which are given to simplify the boundary value problem of the arc region. In addition, the Neumann boundary condition is applied to the upper interface of the arc region.

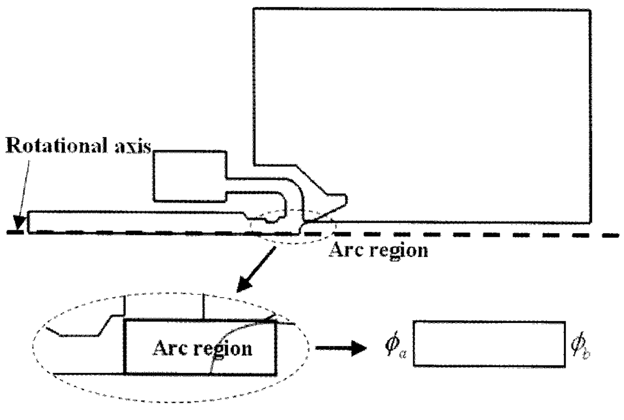

Fig. 1. A certain status of a gas circuit breaker. The area in the oval dotted circle is the arc region (bottom left) and its boundary condition (bottom right).

The electric conductivity of SF_6 gas is affected by circumstances such as temperature and pressure. Even though the state equation for ideal gas explains the relationship of temperature, pressure P, density ρ_g (not to be confused with dilation parameter), and internal energy i such that

$$P = (\gamma - 1)\rho_g i, \quad (10)$$

$$i = e - (|\vec{u}|^2 + |\vec{v}|^2)/2, \quad (11)$$

it does not predict relationships accurately in high temperature plasma [2]. So, after density and internal energy are calculated, we used data from [13] to obtain the conductivity of SF_6 gas as well as temperature and pressure.

For the axisymmetric and inhomogeneous problem, differentiation of the electric conductivity is not vanished, so (7) is rewritten as

$$\frac{\sigma}{r}\frac{\partial\phi}{\partial r} + \sigma\frac{\partial^2\phi}{\partial r^2} + \sigma\frac{\partial^2\phi}{\partial z^2} + \frac{\partial\sigma}{\partial r}\frac{\partial\phi}{\partial r} + \frac{\partial\sigma}{\partial z}\frac{\partial\phi}{\partial z} = 0. \quad (12)$$

Implementation of the FMLSRKM is possible in two ways, such as the Galerkin method and the point collocation scheme. Of the two, we chose the point collocation scheme because the efficiency of the FMLSRKM in the collocation method is better than that of the Galerkin method [4].All nodes in the analysis domain, including interior and boundary nodes,

$$\phi(\mathbf{x}) = \sum_{\mathrm{x}_J \in \Lambda} \phi_J \Psi_J^{[(0,0)]}(\mathrm{x}_J) \quad (13)$$

should be satisfied, and for the nodes in interior node set Λ_i, the point collocation formulation of (12) is

$$\sum_{\mathrm{x}_J \in \Lambda} \phi_J[\sigma(\mathrm{x}_J)\{\Psi_J^{[(2,0)]}(\mathrm{x}_J) + \Psi_J^{[(0,2)]}(\mathrm{x}_J) + \Psi_J^{[(1,0)]}(\mathrm{x}_J)/r\}$$
$$+\sigma_r(\mathrm{x}_J)\Psi_J^{[(1,0)]}(\mathrm{x}_J) + \sigma_z(\mathrm{x}_J)\Psi_J^{[(0,1)]}(\mathrm{x}_J)] = 0 \quad (14)$$
$$\text{for all } x_I \in \Lambda_i$$

where

$$\sigma_r(\mathrm{x}_J) = \left.\frac{\partial\sigma}{\partial r}\right|_{\mathrm{X}=\mathrm{X}_J}, \quad \sigma_z(\mathrm{x}_J) = \left.\frac{\partial\sigma}{\partial z}\right|_{\mathrm{X}=\mathrm{X}_J}, \quad (15)$$

and, for the nodes in boundary node sets Λ_d and Λ_n are also point collocated as

$$\phi_I = g(\mathrm{x}_I) \qquad \text{for all } x_I \in \Lambda_d \quad (16)$$

$$\sum_{x_J \in \Lambda} \phi_J(\Psi_J^{[(1,0)]}(\mathrm{x}_I), \Psi_J^{[(0,1)]}(\mathrm{x}_I)) \bullet \mathbf{n}(\mathrm{x}_I)) = 0 \quad (17)$$
$$\text{for all } x_I \in \Lambda_n$$

where, $\Lambda = \Lambda_i \cup \Lambda_d \cup \Lambda_n$, $\mathbf{n}(\mathrm{x}_I)$ is the outward unit normal vector at $\mathrm{x}_I \in \Lambda_n$, and $\Psi_J^{[\alpha]}(\mathrm{x}_J)$ is α -th shape function which means α -th derivative of the shape function [3], [10]. As seen in (14), for the point collocation method, high-order derivatives up to the order of the governing equation are needed. However, evaluation of the derivatives of the shape function and solution is, numerically, a heavy burden. Consequently, in this paper, we used the FMLSRKM for analysis of an electric field on the arc region because one of its advantages is its ability to calculate derivatives of the shape function, simultaneously [3], [4]. Then, α -th derivative of the approximated solution in the FMLSRKM method can be represented using the shape function as

$$
\begin{aligned}
D^{\alpha}\phi(\mathbf{x}) &= \lim_{\bar{\mathbf{x}}\to\mathbf{x}} D^{\alpha}\phi^{h}(\mathbf{x},\bar{\mathbf{x}}) \\
&= \frac{\alpha!}{\rho^{|\alpha|}}\mathbf{e}_{\alpha}^{T}M^{-1}(\mathbf{x})\sum_{I=1}^{NP}\mathbf{P}_{m}\left(\frac{\mathbf{x}_{I}-\bar{\mathbf{x}}}{\rho}\right)\Phi_{\rho}(\mathbf{x}_{I}-\bar{\mathbf{x}})\phi(\mathbf{x}_{I}) \qquad (18)\\
&= \sum_{I=1}^{NP}\Psi_{I}^{[\alpha]}u(\mathbf{x}_{I}),
\end{aligned}
$$

where, $\mathbf{e}_{\alpha}=(1,0)^{T}$ or $(0,1)^{T}$, $\alpha=(\alpha_1,\alpha_2)$, and $D^{\alpha}=\partial_r^{\alpha_1}\partial_z^{\alpha_2}$. Using the FMLSRKM, it is also convenient to calculate the electric field $\vec{E}$ because derivatives with respect to r and z are obtained as well as the electric potential.

2.3 Analysis of Arc Gas Flow

Euler's equations govern a flow of compressible and inviscid fluid [12]. Using this governing equation, in this paper the arc gas flow is analyzed by finite volume fluid in the cell (FVFLIC) in an axisymmetric coordinate. According to Euler's equations, mass, momentum, and energy are conserved as

$$\frac{\partial\rho_g}{\partial t}+\frac{\partial(\rho_g ur)}{r\partial r}+\frac{\partial(\rho_g v)}{\partial z}=0, \qquad (19)$$

$$\frac{\partial\rho_g u}{\partial t}+\frac{\partial(\rho_g u^2 r)}{r\partial r}+\frac{\partial(\rho_g uv)}{\partial z}=-\frac{\partial(pr)}{r\partial r}, \qquad (20)$$

$$\frac{\partial\rho_g v}{\partial t}+\frac{\partial(\rho_g uvr)}{r\partial r}+\frac{\partial(\rho_g v^2)}{\partial z}=-\frac{\partial(p)}{\partial z}, \qquad (21)$$

$$\frac{\partial E}{\partial t}+\frac{\partial(\rho_g uEr)}{r\partial r}+\frac{\partial(\rho_g vE)}{\partial z}=-\frac{\partial(pur)}{r\partial r}-\frac{\partial(pv)}{\partial z}+S_e, \qquad (22)$$

where, ρ_g is the density of gas, p is pressure, E is the total energy, S_e is the energy source, u and v are the vector components of r and z, respectively [2]. Energy source S_e can be acquired as

$$S_e = S_{ohm} - U_{rad}, \qquad (23)$$

where, U_{rad} is the radiation transport. S_{ohm} is the ohmic heating source and expressed as

$$S_{ohm}=\sigma\,|\vec{E}|^2. \qquad (24)$$

3. Result

An example is shown in Fig. 2. Because there very little analytic solutions for problems on an arc region, the FMLSRKM solution in this example is compared to that of the finite element method (FEM) which is popular as a means of solving various kinds of differential equations. Fig. 2(a) shows the distribution of electric conductivity and, as it shows, inhomogeneity is not negligible. Mesh data for the FEM and node set for the FMLSRKM are represented in Figs. 2(b) and (c), respectively. For comparison of the two methods, nodes in Fig. 2(b) have identical positions with nodes in Fig. 2(c). In Fig. 3, a comparison of the two methods is shown, and Figs. 3(a) and (b) show the electric potentials acquired by the FMLSRKM and FEM, respectively. They show similar results, and it can be seen that the potentials furthest from the axis are distorted due to the conductivity in Fig. 2(a). Figs. 3(c) and (d) are electric field intensities from the FMLSRKM and the FEM, respectively. Although the electric field intensities of the FMLSRKM and the FEM in the area furthest from the axis show little difference, directions and trends of the two results are similar. Fig. 4. shows an example of gas flow in the GCB, and as can be seen, the gas from the cylinder goes to both sides of the arc region.

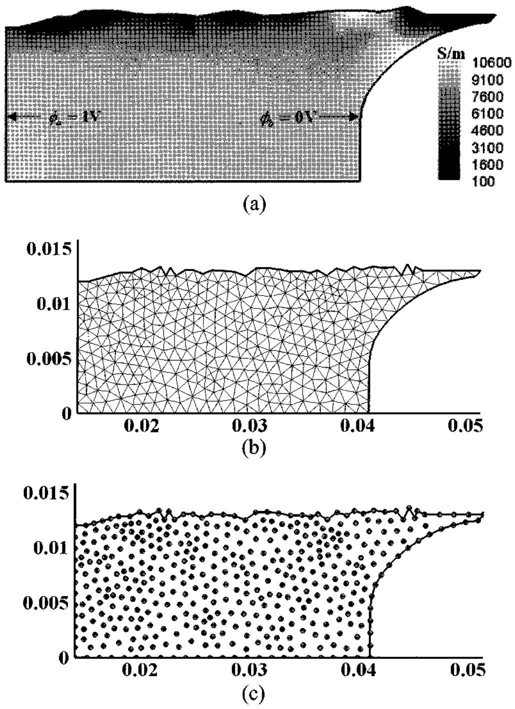

Fig. 2. An example of an arc region analysis. (a) Inhomogeneous electric conductivity is distributed, and Dirichlet boundary conditions are given on sides of the analysis domain. (b) and (c) are mesh data and the node set of the arc region of the finite element method. For comparison of these two methods, nodes in (c) have the same positions of mesh data as in (b). All numbers on axes are in meters.

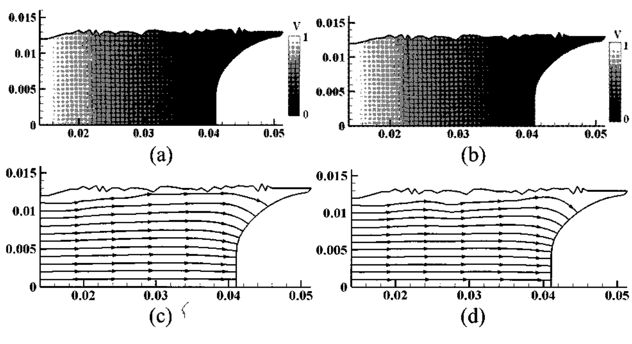

Fig. 3. An example of analysis of electric potential on the arc region. (a) and (b) are potential distributions obtained by the FMLSRKM and FEM, respectively. (c) and (d) are electric field intensities by the FMLSRKM and FEM, respectively. Potential distributions and field intensities from the two methods are similar. All numbers on axes are in meters.

4. Conclusion

Point collocation FMLSRKM for an axisymmetric and inhomogeneous problem is implemented to analyze the electric field of the arc region. In addition to this analysis, arc gas flow estimation described by Euler's equations was implemented using the FVFLIC method. Then, a whole breaking period of GCB is performed by computer simulation. Comparing them to the FEM results of an electric field analysis of the arc region, it is verified that the FMLSRKM can produce an acceptable approximation. Consequently, the FMLSRK method will be a good tool to solve axisymmetric and inhomogeneous problems.

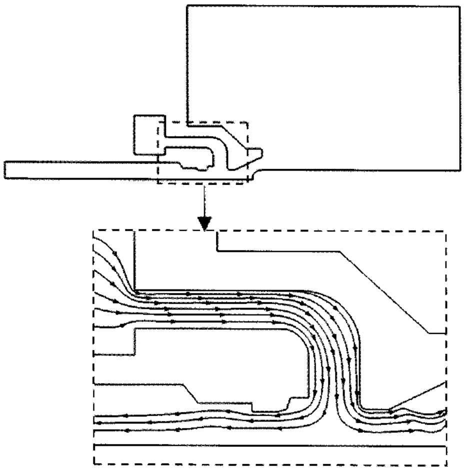

Fig. 4. An example of gas flow in a GCB

References

[1] Bae, C. Y., Jung, H. K., and Choi, K., "Calculation of Small Current Breaking Performance of Gas Circuit Breaker Considering the Real Gas Properties of SF6", *IEEE Trans. Magn*, vol. 41. no.5. pp 1908-1911, 2005.

[2] Park, S. H., Bae, C. Y., Kim, H. K., and Jung, H. K., "Computer simulation of interaction of arc-gas flow in SF6 puffer circuit breaker considering effects of ablated nozzle vapor", *IEEE Trans. Magn.*, vol. 40, no. 4, pp 1067-1070, 2006.

[3] Kim, D. W., and Kim, Y., "Point collocation methods using the fast moving least square reproducing kernel approximation", *Int. J. Numer. Methods. Eng.*, vol. 56, pp 1445-1464, 2003.

[4] Kim, D. W., and Kim, H. K., "Point collocation method based on the FMLSRKM approximation for electromagnetic field analysis", *IEEE Trans. Magn.*, vol. 40, no. 2, pp 1029-1032, 2004.

[5] Gingold, R. A., Monaghan, J. J., "Smoothed particle hydrodynamics: theory and application to nonspherical stars", *Mon. Not. R. astr. Soc.*, vol. 181, pp 375-389, 1997.

[6] Lu, Y. Y., Belytschko, T., and Gu, Lu, "A new implementation of the element free Galerkin method", *Comput. Meth. Appl. Mech. Eng.*, vol. 113, pp 397-414, 1994.

[7] Liu, W. K., Li, S., Belytschko, T., "Moving least square reproducing kernel method (I) methodology and concergence", *Comput. Meth. Appl. Mech. Eng.*, vol. 143, pp 422-433, 1996.

[8] Duarte, C. A., Oden, J. T., "An h-p adaptive method using clouds", *Comput. Meth. Appl. Mech. Eng.*, vol. 139, pp 237-262, 1996.

[9] Liu, W. K., Jun, S., Zhang, Y. F., "Reproducing kernel particle methods", *Int. J. Numer. Meth. Fl.*, vol. 20, pp 1081-1106, 1995.

[10] Lee, C., Im, C. H., Jung, H. K., Kim, H. K., and Kim, D. W., "A Posteriori error estimation and adaptive node refinement for fast moving least square reproducing kernel method", *Comput. Model. Eng. Sci.*, vol. 20, no. 1, pp 35-41, 2007.

[11] Zhang, J. L., Yan, J. D., Murphy, A. B., Hall, W., and Fang, M. T. C., "Computational investigation of arc behavior in an auto-expansion circuit breaker contaminated by ablated nozzle vapor", *IEEE Trans. Plasma Sci.*, vol. 30, no. 4, pp 706-719, 2002.

[12] Hafez, M., "Finite element/finite volume solution of full potential, Euler and Navier-Stokes equations for compressible and incompressible flows", *Int. J. Numer. Meth. Fl.*, vol. 20, pp 713-741, 1995

[13] Liebermann, R. W., and Lowke, J. J., "Radiation emission coefficients for sulfur hexafluoride arc plasmas," *J. Quantum Spectrosc. Radiant. Transfer*, vol. 16, pp 253-264, 1976.

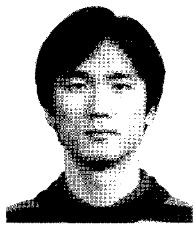

Chany Lee received his B.S. degree in electrical engineering from Seoul National University. His research interests are numerical analysis and neuroelectro-magnetism.

Do Wan Kim received his Ph.D. degree in mathematics from KAIST. His research interests are fluid mechanics and meshfree methods.

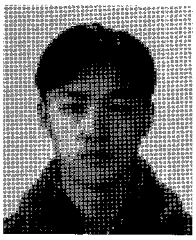

Sang-Hun Park received his Ph.D. degree in electrical engineering from Seoul National University. His research interests are gas circuit breaker and numerical analysis.

Hong-Kyu Kim received his Ph.D. degree in electrical engineering from Seoul National University. His research interests are electric power systems and numerical analysis.

Hyun-Kyo Jung received his Ph.D. degree in electrical engineering from Seoul National University. His research interests are electric machinery, EM wave, circuit breaker, and so on.